ChemComm

ROYAL SOCIETY OF CHEMISTRY

COMMUNICATION

View Article Online
View Journal | View Issue

Cite this: *Chem. Commun.*, 2020, **56**, 8623

Received 27th April 2020,
Accepted 15th June 2020

DOI: 10.1039/d0cc03053h

rsc.li/chemcomm

Phosphorene-quantum-dot-interspersed few-layered MoS_2 hybrids as efficient bifunctional electrocatalysts for hydrogen and oxygen evolution†

Ranjith Prasannachandran, T. V. Vineesh, M. B. Lithin, R. Nandakishore and M. M. Shaijumon *

0-D/2-D hybrids made up of phosphorene quantum dot (PQD)-interspersed few-layered MoS_2 nanosheets were demonstrated to be efficient electrocatalysts with remarkable bifunctional electrocatalytic activity for oxygen and hydrogen evolution in an alkaline medium. The excellent performance of the PQD/MoS_2 hybrids was attributed to their unique morphology, which facilitated charge transfer, leading to improved HER and OER kinetics.

Black phosphorus, a unique two-dimensional material, has recently gained significant attention owing to its interesting physico-chemical properties that make it suitable in diverse applications including optoelectronics, photovoltaics, energy storage, sensing, and catalysis.[1–4] With its tunable electronic properties, large surface area, ultra-thin nature, and structural tailorability, few-layered black phosphorus has recently been studied as a promising electrocatalyst for the hydrogen evolution reaction (HER) and oxygen evolution reaction (OER).[5–8] Several strategies including functionalization and surface engineering have been reported to improve its electrocatalytic activity in terms of overpotential, stability, *etc.* Recently we demonstrated enhanced electrocatalytic activity for functionalized phosphorene quantum dots, prepared using a single-step electrochemical exfoliation method, towards the OER in an alkaline medium.[9] Making heterostructures of 2D materials is a promising strategy proposed to tailor their properties toward specific applications including energy storage and electro/photocatalysis.[7,10–15] Recently, in-plane heterostructures of few-layered black phosphorus with dicobalt and dinickel phosphides have been shown to display improved electrocatalytic properties toward the HER and OER.[16]

The electrocatalysts for both the HER and OER have been recommended to be operated under the same pH range and also in very strong alkaline or acidic media so as to reduce the overpotentials for the purpose of achieving high efficiency for overall water splitting.[17] Thus the realization of a practical and efficient water splitting device requires development of low-cost noble-metal-free electrocatalysts for both the HER and OER. Though there have been significant advances in the development of TMD-, phosphide-, nitride- and carbon-based electrocatalysts, materials that show bifunctionality for the HER and OER, which could thus be employed in reaction cells under the same pH and electrolyte conditions, still remain to be explored. For instance, while TMDs such as mono-/few-layered MoS_2 exhibit exceptional electrocatalytic activity towards the HER in acidic media, close to that of commercial Pt/C, making such TMDs suitable for the same reaction with high efficiency in an alkaline medium or applicable as efficient OER catalysts is quite challenging. Hence there is an urgent need to develop strategies for fabricating hybrid bifunctional electrocatalysts, with engineered interfaces that allow for adsorption of hydrogen-containing and oxygen-containing intermediates, for the realization of economically viable water splitting devices. Herein, we report a simple one-step technique to obtain 0D/2D hybrids consisting of phosphorene quantum dot (PQD)-interspersed few-layered MoS_2 nanosheets, under ambient conditions. The as-synthesized PQD/MoS_2 hybrid exhibited remarkable bifunctional electrocatalytic activity with exceptional stability in an alkaline medium, with an overpotential of 1.60 V@10 mA cm^{-2} towards the OER and −0.6 V@10 mA cm^{-2} towards the HER. The results demonstrated the promising potential of the PQD/MoS_2 hybrid to serve as technologically viable electrodes for the overall water splitting process.

We employed a single-step processing method to prepare 0D/2D hybrids of phosphorene quantum dots (PQDs) interspersed with few-layered MoS_2 nanosheets, following an electrochemical route.[18,19] In a typical process, bulk MoS_2 and BP crystals mixed in a weight ratio of 5 : 1 were thoroughly ground using a mortar and pestle, and then pressed into a pellet and used as an anode in a custom-designed electrochemical cell with conducting substrate

School of Physics, Indian Institute of Science Education and Research Thiruvananthapuram, Maruthamala PO, Thiruvananthapuram, Kerala, 695551, India. E-mail: shaiju@iisertvm.ac.in

† Electronic supplementary information (ESI) available. See DOI: 10.1039/d0cc03053h

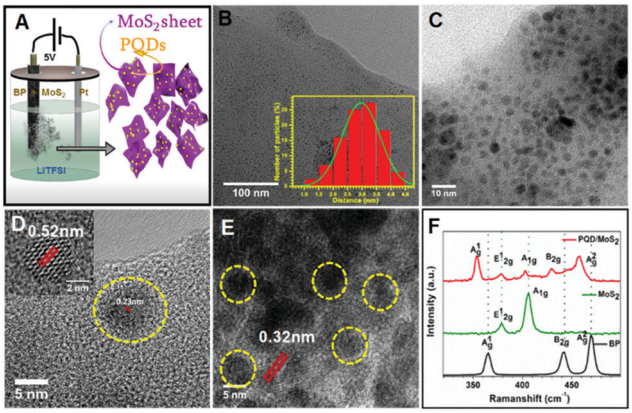

Fig. 1 (A) Schematic showing the electrochemical synthesis of PQD/MoS_2. (B) Low-resolution and (C) high-resolution TEM images of PQD/MoS_2. Inset of (B) shows a histogram of the average particle size distribution of PQDs on MoS_2 sheets. (D) HRTEM image of PQD/MoS_2 with a PQD highlighted and revealing lattice fringes (interlayer spacing of 0.23 nm) on the MoS_2 nanosheet. The inset of (D) shows an HRTEM image of a PQD with highly resolved lattice fringes. (E) HRTEM image of PQD/MoS_2 showing the lattice fringes of MoS_2 with an interlayer spacing of 0.32 nm. (F) Raman spectra of PQD/MoS_2 heterostructures and their bulk counterparts.

(FTO/Pt wire) as the cathode. A highly dispersed solution of PQD/MoS_2 heterostructures was obtained when a 5 V DC potential was applied under ambient conditions for 6 h between the electrodes in an aqueous electrolyte composed of 0.1 wt% LiTFSI (Fig. 1A), as detailed in the Experimental section (ESI†). The obtained light-greenish solution was centrifuged at 5000 rpm for 15 min and the collected dispersion showed the presence of 0D/2D heterostructures, as confirmed from a UV-Vis absorption spectrum showing a sharp peak at a wavelength of 300 nm and corresponding to the characteristic absorption band of PQDs, and a broad peak at 610 nm and corresponding to that of few-layered MoS_2 sheets (Fig. S1, ESI†).[18,20,21] Pumera and co-workers have earlier reported the electrochemical exfoliation of black phosphorus in aqueous Na_2SO_4.[19] In our current work, aqueous LiTFSI was chosen as a better candidate—as the TFSI ions, being bigger, were expected to facilitate exfoliation by intercalating into the spacing between the weakly-held-together van der Waals layers of these materials, and in this location to then trigger the cleavage and exfoliation.

The morphology of the heterostructures was examined by carrying out transmission electron microscopy (TEM). Inspection of the TEM image of PQD/MoS_2, shown in Fig. 1B, revealed the presence of nearly monodisperse quantum dots that were well interspersed on ultra-thin sheets. Further characterization using high-resolution TEM (Fig. 1C–E and Fig. S2, ESI†) revealed the MoS_2 sheets to have dimensions of several hundred nanometers and the well interspersed PQDs to have average lateral dimensions of ~3 nm (inset of Fig. 1B) with an average height of 3–4 nm (Fig. S3, ESI†). Inspection of the acquired HRTEM image of the PQD particles revealed lattice fringes with interlayer spacings of 0.52 nm and 0.23 nm (Fig. 1D), corresponding to the (020) and (111) planes of the bulk black phosphorus crystal.[4,22,23] Inspection of the acquired HRTEM image of the nanosheets clearly showed lattice fringes with an interplanar distance of 0.32 nm (Fig. 1E) and that corresponded to the (004) plane of the MoS_2 sheets. This result confirmed the formation of the 0D/2D heterostructure, one held together purely based on electrostatic attraction.

A Raman spectrum recorded for the currently developed heterostructure sample showed characteristic Raman signals for both MoS_2 and black phosphorus, clearly confirming the heterostructure formation (Fig. 1F). The peaks at 353.6 cm^{-1}, 430 cm^{-1}, and 458.2 cm^{-1} corresponded to the three vibrational modes of black phosphorus (A_g^1, B_{2g}, and A_g^2, respectively).[5,24–26] The Raman signatures for MoS_2 were observed in the form of the characteristic peaks (E_{2g}^1 and A_g^2) observed at 378.5 cm^{-1} and 402.7 cm^{-1}. The difference between the wavenumber of the E_{2g}^1 peak and that of the A_g^2 peak was measured to be 24 cm^{-1}, which confirmed the presence of exfoliated few-layer MoS_2.[5] The characteristic Raman peaks observed for PQDs and MoS_2 showed a redshift from their pristine bulk counterparts, which might have been due to electron transfer at the PQD/MoS_2 interface, as observed for other 2D heterostructures reported earlier.[5] To further confirm the heterostructure formation based on elemental analysis, scanning transmission electron microscopy with electron energy loss spectroscopy mapping (STEM-EELS) was performed on the sample, as shown in Fig. S4 (ESI†). The energy losses recorded from the sheet for the S $L_{2,3}$ edge at ~165 eV and the Mo $M_{4,5}$ edge at ~230 eV were attributed to, respectively, the excitation of the $2p_{3/2}$ and $2p_{1/2}$ electrons to unoccupied 3d states and the excitation of the $3d_{5/2}$ and $3d_{3/2}$ electrons to unoccupied 4d states in the MoS_2.[27] The presence of phosphorene particles on the MoS_2 sheets was further confirmed by the observation of the P $L_{2,3}$ edge.[28] Control experiments were performed with bulk MoS_2 and black phosphorus anodes separately under similar conditions to confirm the formation of MoS_2 sheets and PQDs, respectively (Fig. S5, ESI†). X-ray photoelectron spectroscopy (XPS) measurements were further taken to study the chemical composition of the material (Fig. S6, ESI†). The XPS survey spectrum recorded for the heterostructure sample showed peaks corresponding to Mo, S, and P, as expected (Fig. S6A, ESI†). The presence of adventitious C and O was also seen. The deconvoluted high-resolution Mo 3d spectra showed characteristic peaks at 236.3 eV and 233.2 eV, corresponding to Mo $3d_{3/2}$ and Mo $3d_{5/2}$ signatures, respectively (Fig. S6B, ESI†). Slight shifts in the peaks compared to bulk MoS_2 towards higher binding energy resulted from the oxidized edge of MoS_2 sheets arising from the applied anodic potential in the aqueous medium.

A high-resolution deconvoluted XPS spectrum in the S 2p region showed signature S–O peaks, confirming a slight oxidation of MoS_2 nanosheets (Fig. S6C, ESI†). The deconvoluted high-resolution spectrum in the P 2p region showed two peaks (Fig. S6D, ESI†), one observed at ~135 eV and corresponding to highly oxidized PQDs, and the other peak at ~130 eV and corresponding to the P–P bond of phosphorene. The 135 eV peak corresponding to the P_xO_y bond resulted from the anodic exfoliation process in the presence of an aqueous electrolyte.[19,29] It should be noted that no peaks corresponding to Mo–P bonds were observed in the P 2p and Mo 3d XPS regions, clearly indicating purely electrostatic binding between the two species

with the van der Waals force driving the formation of the PQD/MoS_2 heterostructure. Owing to the unique morphology of the 0D/2D heterostructure that facilitated improved interfacial contact and electronic interaction, our major goal here was to explore the bifunctional electrocatalytic activity of PQD/MoS_2 heterostructures as efficient OER and HER catalysts for the overall water splitting process. Mono-/few-layered black phosphorus upon functionalization and surface engineering through diverse strategies has been shown to exhibit improved OER activity. For instance, in one of our previous works, *in situ*-surface-functionalized PQDs with nitrogen-containing groups were shown to exhibit efficient and stable electrocatalytic activity for the OER.[9] Mono-/few-layered MoS_2 is a well-explored electrocatalyst exhibiting exceptional activity towards the HER in acidic media, but its HER performance in alkaline media is very poor, limiting its practical use for overall water splitting devices. We thus thought it would be interesting to investigate the HER and OER activities of PQD/MoS_2 heterostructures in an alkaline medium, from a practical standpoint.

The OER activity of PQD/MoS_2 heterostructures was evaluated in 0.1 M KOH, as were bulk MoS_2, few-layered MoS_2 sheets, bulk BP and PQDs for comparison. All of the potentials were converted to the reversible hydrogen electrode (RHE) and iR compensation was applied while recording the data using a Bio-logic SAS VMP3 workstation. Fig. 2A shows the linear sweep voltammetry curves obtained for determining the OER activities of the various samples. While both bulk MoS_2 and bulk BP showed poor OER performances, the heterostructure showed exceptional OER activity, with an overpotential of only 1.60 V at 10 mA cm^{-2}, lower than the overpotentials of the other tested samples. The PQDs showed a slight enhancement in OER performance compared to bulk BP, which could be attributed to their increased quantity of edge sites. An OER catalyst is in general considered to be efficient if its overpotential and Tafel slope are low and its exchange current density is high. Apart from the Tafel slope, analyzing an impedance spectrum (EIS) also gives information regarding the rate-determining step, and hence regarding the OER kinetics of the catalyst. In an alkaline medium, oxygen evolution undergoes a multistep reaction process to convert OH^- to O_2. The first step of an OER is an electron transfer process where the relevant Tafel slope has been shown to be 120 mV dec^{-1}. In the second step, the Tafel slope can be either 60 mV dec^{-1} or 40 mV dec^{-1}, depending on whether a chemical reaction or an electron–proton reaction is the rate-limiting step.[30,31] The PQD/MoS_2 heterostructures exhibited excellent OER activity with a low Tafel slope of 46 mV dec^{-1} (Fig. 2B), suggesting improved kinetics due to accumulation of electrons on the heterojunction for a faster electron–proton reaction. Furthermore, analysis of the Nyquist plots revealed an impedance of 46 Ohm for PQD/MoS_2, much lower than those of the other samples (Fig. 2C), and revealing a lower charge-transfer resistance and faster faradaic process in the heterostructure material. Electrode stability is another key parameter, and the as-prepared PQD/MoS_2 was found to be stable for more than 15 h at a potential of 1.65 V (Fig. 2D), indicating excellent durability of the material in alkaline medium.

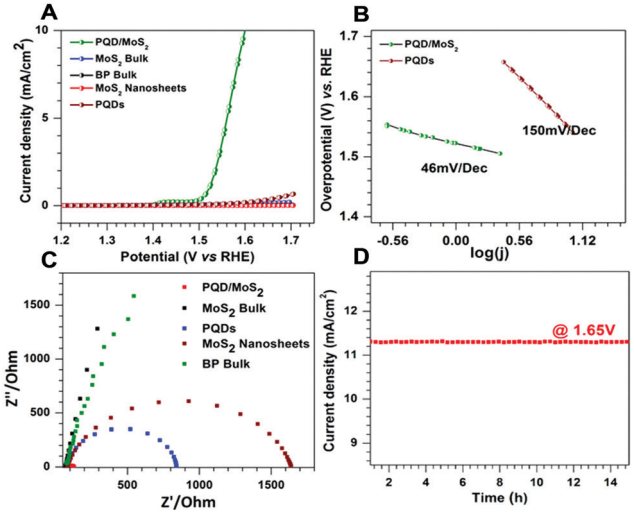

Fig. 2 (A) LSVs acquired for determining the OER activities of various samples in 0.1 M KOH solutions at 1600 rpm. (B) Tafel plots of PQD/MoS_2 and PQDs measured from the corresponding LSVs in (A). (C) Impedance spectra of PQD/MoS_2 and of the other indicated samples. (D) Chronoamperometric response of PQD/MoS_2, indicating their long-term durability.

The overall OER performance of the PQD/MoS_2 heterostructures was found to be on par with those of other recently reported bifunctional electrocatalysts (Table S1, ESI†).

The HER activities of PQD/MoS_2 and the other samples were evaluated in 0.1 M KOH under similar conditions (Fig. 3). Mono-/few-layered MoS_2 has been extensively studied as a highly efficient electrocatalyst for the HER in acidic medium, and hence we thought it would be further interesting to investigate the HER activity of the heterostructure sample consisting of exfoliated MoS_2 sheets, in an alkaline medium. In general, the formation of heterostructures or nanohybrids induces a negative electric field between dissimilar layers, which further enhances the adsorption of H^+ onto the catalyst, a well-studied mechanism for MoS_2/graphene nanohybrids.[12] We had thought that electron injection from PQD to MoS_2 would favor the stabilization of adsorbed H over the surface, and as a consequence would enhance the HER activity. Also, the heterogeneous atoms can give a close thermoneutral free energy ($\Delta G \sim 0$) for hydrogen evolution reaction.[32] As evidenced from the LSV curves in Fig. 3A, PQD/MoS_2 showed a much better HER activity than did bulk BP, PQDs, bulk MoS_2, and the exfoliated MoS_2 nanosheets. PQD/MoS_2 exhibited here an overpotential of ~ -0.6 V at 10 mA cm^{-2}, much better than that of the exfoliated MoS_2 nanosheets (Fig. 3A). Furthermore, a much lower Tafel slope, specifically 162 mV dec^{-1}, was measured for PQD/MoS_2 than for the other samples (Fig. 3B). A much smaller semicircle observed in the impedance plot (Fig. 3C) indicated improved charge-transfer kinetics for PQD/MoS_2, which could be due to the faster electron transfer through the heterojunction. Such faster electron transfer would further result in enhanced coupling of an electron with H^+ ions at the catalyst-electrolyte interface. The long-term stability of the heterostructure was also confirmed from the electrochemical amperometry measurements performed at a potential

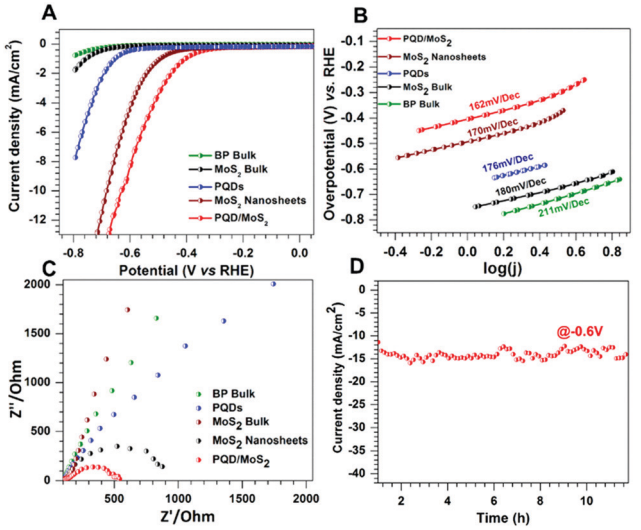

Fig. 3 (A) LSV curves acquired for determining the HER activities of various samples in 0.1 M KOH solutions at 1600 rpm. (B) Tafel plots obtained from the corresponding LSVs in (A). (C) Impedance spectra of samples. (D) Chrono-amperometric response of PQD/MoS_2, revealing the long-term durability of the heterostructure.

of −0.6 V *vs.* RHE for more than 15 h (Fig. 3D). Furthermore, the structural stability of the catalyst after electrocatalytic measurements was confirmed from Raman (Fig. S9, ESI†) and XPS (Fig. S10, ESI†) analyses.

In summary, we have shown a facile and one-step electrochemical approach to make 0D/2D hybrids of PQD/MoS_2 under ambient conditions. As-prepared PQD/MoS_2 exhibited remarkable bifunctional electrocatalytic activity towards the HER and OER in a 0.1 M KOH solution. The bifunctional catalyst also showed exceptional stability in an alkaline medium, with an overpotential of 1.60 V@10 mA cm^{-2} towards the OER and −0.6 V@10 mA cm^{-2} towards the HER with very low Tafel slopes. The enhanced electrocatalytic performance of MoS_2/PQDs was attributed to its unique morphology, with monodisperse PQDs uniformly interspersed on few-layered MoS_2 nanosheets, and with this morphology facilitating charge transfer and hence leading to improved HER and OER kinetics. The importance of design strategies for the development of 0D/2D hybrids to meet the requirements of both hydrogen and oxygen evolution electrocatalysts was highlighted using detailed electrochemical studies and the work thus brings us a step closer to the realization of a practical water splitting system.

Conflicts of interest

There are no conflicts to declare.

Notes and references

1 D. Hanlon, C. Backes, E. Doherty, C. S. Cucinotta, N. C. Berner, C. Boland, K. Lee, A. Harvey, P. Lynch and Z. Gholamvand, *et al.*, *Nat. Commun.*, 2015, **6**, 8563.
2 F. Xia, H. Wang and Y. Jia, *Nat. Commun.*, 2014, **5**, 4458.
3 Z. Guo, H. Zhang, S. Lu, Z. Wang, S. Tang, J. Shao, Z. Sun, H. Xie, H. Wang and X.-F. Yu, *et al.*, *Adv. Funct. Mater.*, 2015, **25**, 7100.
4 X. Ren, J. Zhou, X. Qi, Y. Liu, Z. Huang, Z. Li, Y. Ge, S. C. Dhanabalan, J. S. Ponraj and S. Wang, *et al.*, *Adv. Energy Mater.*, 2017, **7**, 1700396.
5 R. He, J. Hua, A. Zhang, C. Wang, J. Peng, W. Chen and J. Zeng, *Nano Lett.*, 2017, **17**, 4311–4316.
6 L. Shao, H. Sun, L. Miao, X. Chen, M. Han, J. Sun, S. Liu, L. Li, F. Cheng and J. Chen, *J. Mater. Chem. A*, 2018, **6**, 2494–2499.
7 Y. Lin, Y. Pan and J. Zhang, *Int. J. Hydrogen Energy*, 2017, **42**, 7951–7956.
8 Y. Gan, X.-X. Xue, X.-X. Jiang, Z. Xu, K. Chen, J.-F. Yu and Y. Feng, *J. Phys.: Condens. Matter*, 2019, **32**, 25202.
9 R. Prasannachandran, T. V. Vineesh, A. Anil, B. M. Krishna and M. M. Shaijumon, *ACS Nano*, 2018, **12**, 11511–11519.
10 Z. Yuan, J. Li, M. Yang, Z. Fang, J. Jian, D. Yu, X. Chen and L. Dai, *J. Am. Chem. Soc.*, 2019, **141**, 4972–4979.
11 T. Wu, S. Zhang, K. Bu, W. Zhao, Q. Bi, T. Lin, J. Huang, Y. Li and F. Huang, *J. Mater. Chem. A*, 2019, **7**, 22063–22069.
12 J. Ye, W. Chen, S. Xu, Z. Yu and S. Hou, *RSC Adv.*, 2016, **6**, 104925.
13 Q. Liang, F. Shi, X. Xiao, X. Wu, K. Huang and S. Feng, *ChemCatChem*, 2018, **10**, 2179–2183.
14 S. Bawari, N. M. Kaley, S. Pal, T. V. Vineesh, S. Ghosh, J. Mondal and T. N. Narayanan, *Phys. Chem. Chem. Phys.*, 2018, **20**, 15007–15014.
15 J. Wang, D. Liu, H. Huang, N. Yang, B. Yu, M. Wen, X. Wang, P. K. Chu and X.-F. Yu, *Angew. Chem., Int. Ed.*, 2018, **57**, 2600–2604.
16 Z.-Z. Luo, Y. Zhang, C. Zhang, H. T. Tan, Z. Li, A. Abutaha, X.-L. Wu, Q. Xiong, K. A. Khor and K. Hippalgaonkar, *et al.*, *Adv. Energy Mater.*, 2017, **7**, 1601285.
17 Y. Yan, B. Y. Xia, B. Zhao and X. Wang, *J. Mater. Chem. A*, 2016, **4**, 17587–17603.
18 D. Gopalakrishnan, D. Damien, B. Li, H. Gullappalli, V. K. Pillai, P. M. Ajayan and M. M. Shaijumon, *Chem. Commun.*, 2015, **51**, 6293–6296.
19 A. Ambrosi, Z. Sofer and M. Pumera, *Angew. Chem., Int. Ed.*, 2017, **56**, 10443–10445.
20 A. K. Mishra, K. V. Lakshmi and L. Huang, *Sci. Rep.*, 2015, **5**, 15718.
21 Z. Guo, H. Zhang, S. Lu, Z. Wang, S. Tang, J. Shao, Z. Sun, H. Xie, H. Wang and X.-F. Yu, *et al.*, *Adv. Funct. Mater.*, 2015, **25**, 6996–7002.
22 Z. Guo, H. Zhang, S. Lu, Z. Wang, S. Tang, J. Shao, Z. Sun, H. Xie, H. Wang and X.-F. Yu, *et al.*, *Adv. Funct. Mater.*, 2015, **25**, 6996–7002.
23 X. Zhang, H. Xie, Z. Liu, C. Tan, Z. Luo, H. Li, J. Lin, L. Sun, W. Chen and Z. Xu, *et al.*, *Angew. Chem., Int. Ed.*, 2015, **127**, 3724–3728.
24 J. R. Brent, N. Savjani, E. A. Lewis, S. J. Haigh, D. J. Lewis and P. O'Brien, *Chem. Commun.*, 2014, **50**, 13338–13341.
25 Z. Sun, H. Xie, S. Tang, X.-F. Yu, Z. Guo, J. Shao, H. Zhang, H. Huang, H. Wang and P. K. Chu, *Angew. Chem., Int. Ed.*, 2015, **127**, 11688–11692.
26 X. Zhang, H. Xie, Z. Liu, C. Tan, Z. Luo, H. Li, J. Lin, L. Sun, W. Chen and Z. Xu, *et al.*, *Angew. Chem., Int. Ed.*, 2015, **127**, 3724–3728.
27 D. Dahanayake, S. Gunasekara, V. Jayaweera, C. Sandaruwan, V. Karunarathne and G. A. J. Amaratunga, *CrystEngComm*, 2018, **20**, 6482–6489.
28 X. Liu, J. D. Wood, K.-S. Chen, E. Cho and M. C. Hersam, *J. Phys. Chem. Lett.*, 2015, **6**, 773–778.
29 C. C. Mayorga-Martinez, N. Mohamad Latiff, A. Y. S. Eng, Z. Sofer and M. Pumera, *Anal. Chem.*, 2016, **88**, 10074–10079.
30 J. O. Bockris, *J. Chem. Phys.*, 1956, **24**, 817–827.
31 N.-T. Suen, S.-F. Hung, Q. Quan, N. Zhang, Y.-J. Xu and H. M. Chen, *Chem. Soc. Rev.*, 2017, **46**, 337–365.
32 Y. Zheng, Y. Jiao, L. H. Li, T. Xing, Y. Chen, M. Jaroniec and S. Z. Qiao, *ACS Nano*, 2014, **8**, 5290–5296.

